0026-895X/08/7301-18–26$20.00
MOLECULAR PHARMACOLOGY
Copyright © 2008 The American Society for Pharmacology and Experimental Therapeutics
*Mol Pharmacol* 73:18–26, 2008

Vol. 73, No. 1
35519/3286916
*Printed in U.S.A.*



# Stretch Induction of Cyclooxygenase-2 Expression in Human Urothelial Cells Is Calcium- and Protein Kinase C ζ-Dependent

Travis J. Jerde, William S. Mellon, Dale E. Bjorling, Celina M. Checura, Kwadwo Owusu-Ofori, John J. Parrish, and Stephen Y. Nakada

*The Uropharmacology and Endourology Research Laboratory; Departments of Pharmaceutical Sciences (T.J.J., W.S.M.), School of Veterinary Medicine (C.M.C., D.E.B.), College of Agricultural and Life Sciences (J.J.P.), and Surgery-Division of Urology (T.J.J., D.E.B., S.Y.N.), University of Wisconsin School of Medicine and Public Health, Madison, Wisconsin*

Received April 6, 2007; accepted October 9, 2007

## ABSTRACT

Prostanoid synthesis via cyclooxygenase (COX)-2 induction during urothelial stretch is central to nociception, inflammation, contractility, and proliferation caused by urinary tract obstruction. We used our primary human urothelial cell stretch model published previously to evaluate the signaling mechanisms responsible for stretch-induced COX-2 expression in urothelial cells. To determine intracytosolic calcium concentrations ($[Ca^{2+}]_i$), primary human urothelial cells were grown on flexible membranes and loaded with Fura-2 acetoxymethyl ester (AM). We determined $[Ca^{2+}]_i$ using a fluorescent scope during stretch. Additional cells were treated with 1,2-bis(2-aminophenoxy)ethane-*N*,*N*,*N*′,*N*′-tetraacetic acid (BAPTA)-AM, stretched, and COX-2 mRNA and protein were evaluated by real-time polymerase chain reaction and immunoblotting. To evaluate protein kinase C (PKC) in this system, cells were stretched and fractionated into membrane, cytosol, and nucleus. Fractions were immunoblotted for PKCα, β1, and ζ, the predominant isoforms in urothelial cells. We treated additional cells with increasing concentrations of either bisindolylmaleimide-I or a peptide PKC pseudosubstrate inhibitor, and COX-2 mRNA and protein were evaluated after stretching. Furthermore, we transfected urothelial cells with siRNA against each of the inducible PKC isoforms in these cells and evaluated the stretch-induced COX-2 response. Stretch of urothelial cells activated calcium flux and PKC translocation to membrane and nucleus. Pharmacological inhibition indicated that stretch-induced COX-2 expression is dependent on calcium and PKC, and biochemical knockdown experiments indicated that PKCζ is the predominant isoform mediating stretch-induced COX-2 expression. Elucidating the signaling mechanism of stretch-induced COX-2 expression may identify therapeutic targets.

Obstructive diseases of the ureter are associated numerous deleterious effects including severe pain, inflammation, hypercontractility, cell proliferation, and potentially cell transformation (Gulmi et al., 1998; Weiss, 1998). Ureteral obstruction has a lifetime incidence of 13%, and total societal costs associated with diagnosis, treatment, pain management, and lost wages total more than $2 billion annually (Clark et al., 1995; Ramello et al., 2000). There is a substantial gap in the knowledge of the physiological changes that occur during ureteral obstruction, and this has limited the development of superior pharmacological agents for symptomatic treatment of the disease. Because of this, narcotics remain first-line therapy for treatment of symptomatic ureteral obstruction, despite serious side effects and addictive concerns.

Prostanoids are critical to the physiological effects associated with ureteral obstruction (Cole et al., 1988). The rate-limiting step in prostanoid synthesis is conversion of arachidonic acid to prostaglandin $G_2$ and subsequent conversion to prostaglandin $H_2$. (Foegh et al., 1999) This reaction is catalyzed by cyclooxygenase (COX), an enzyme that exists in two isoforms: COX-1 and COX-2 (Kujubu et al., 1991). COX-1 is present in most human tissues, and although COX-1 expression can be regulated, it is usually considered to be expressed constitutively (Foegh et al., 1999). COX-2 is present in most tissues at low levels but is substantially induced by local inflammatory and physical stimuli in addition to its homeostatic role.

Nonsteroidal anti-inflammatory drugs inhibit prostanoid

Article, publication date, and citation information can be found at http://molpharm.aspetjournals.org.
doi:10.1124/mol.107.035519.

**ABBREVIATIONS:** COX, cyclooxygenase; PKC, protein kinase C; AM, acetoxymethyl ester; GAPDH, glyceraldehyde-3-phosphate dehydrogenase; DTT, dithiothreitol; PP, psuedosubstrate peptide; PBS, phosphate-buffered saline; DMSO, dimethyl sulfoxide; BAPTA, 1,2-bis(2-aminophenoxy)ethane-*N*,*N*,*N*′,*N*′-tetraacetic acid; TEDK, Tris-HCl/KCl/EDTA/dithiothreitol/protease inhibitor cocktail; siRNA, small interfering RNA; KT-5720, (9*S*,10*S*,12*R*)-2,3,9,10,11,12-hexahydro-10-hydroxy-9-methyl-1-oxo-9,12-epoxy-1*H*-diindolo[1,2,3-*fg*:3′,2′,1′-*kl*]pyrrolo[3,4-*i*][1,6]benzodiazocine-10-carboxylic acid hexyl ester.

synthesis and are used effectively to treat the pain and inflammation associated with urological obstruction (Baçsar et al., 1991). However, nonsteroidal anti-inflammatory drugs cause gastric ulceration, inhibit platelet aggregation, and impair renal function (Oren and Ligumsky, 1994; Colletti et al., 1999). Selective COX-2 blockade is an intriguing therapy for symptoms of urinary tract obstruction because these medications provide potent analgesia with fewer toxic side effects than nonselective COX inhibitors (Lanza et al., 1999). However, selective COX-2 inhibitors are also associated with renal side effects, particularly during ureteral obstruction when renal function is compromised (Brune and Neubert, 2001; Hernández et al., 2002). In addition, COX-2 inhibition is associated with cardiovascular side effects and clotting in susceptible individuals (Mukherjee et al., 2001). Elucidation of cellular mechanisms that couple distention of the urinary tract with increased COX-2 activity may identify targets of drug action directed specifically at COX-2 induction.

In vivo obstruction and distension induces COX-2 expression in the urinary bladder, ureter, and kidney (Park et al., 1997; Nakada et al., 2002; Chou et al., 2003). Furthermore, mechanical stretch induces COX-2 expression in numerous cell culture models, including vascular endothelial cells, osteoblasts, and renal podocytes (Inoue et al., 2002; Fitzgerald et al., 2004; Martineau et al., 2004). In addition, we have reported recently a cell culture model of urothelial cell stretch-induced COX-2 expression and found that stretch-induced COX-2 expression is regulated at both transcriptional and post-transcriptional levels (Jerde et al., 2006).

We seek to determine the cellular mechanosensitive pathways in urothelial cells responding to during stretch that result in COX-2 induction. Deciphering the signaling mechanisms will assist in the identification of novel drug targets for the treatment of symptomatic urological obstructions. Stretch-activated calcium flux is believed to be a trigger in cellular stretch signaling (Hamill and Martinac, 2001). A primary effect of calcium signaling is activation of protein kinase C (PKC) signaling, and recent reports have implicated PKC as critical in mechanotransduction (Malhotra et al., 2001). The 11 known isoforms of PKC are divided into four major groups: classic ($\alpha$, $\beta$1, $\beta$2, $\gamma$), novel ($\delta$, $\varepsilon$, $\eta$, $\theta$), atypical ($\zeta$, $\iota/\lambda$), and $\mu$ (Newton, 1995). Upon activation by calcium, classic PKC isoforms migrate to the plasma membrane or nucleus and are active as kinases (Newton, 1995). The purpose of this study is to determine whether cell stretch induces calcium flux and PKC activation (translocation) and to determine whether these signaling intermediates are involved in stretch-induced COX-2 expression.

## Materials and Methods

**Pharmacological Agents and Chemicals.** Ham's F-12 nutrient medium, streptomycin/penicillin, fetal bovine serum, L-glutamine, glucose, transferrin, nonessential amino acids, and trypsin-EDTA were purchased from Sigma-Aldrich (St. Louis, MO). Fura-2 AM, Fura-2, and the medium calcium removal kit were purchased from Invitrogen (Carlsbad, CA). BAPTA-AM, bisindolylmaleimide-1, myristoylated PKC pseudosubstrate peptide, and KT-5720 were purchased from Calbiochem (La Jolla, CA). GAPDH monoclonal antibody was purchased from Abcam (Cambridge, MA), and COX-2 monoclonal antibody was purchased from Cayman Chemical (Ann Arbor, MI). Polyclonal antibodies to all PKC isoforms were purchased from Santa Cruz Biotechnology (Santa Cruz, CA). Antibodies to nuclear lamin B1 and lactate dehydrogenase were purchased from Abcam, and the adenylyl cyclase activity assay was purchased from Molecular Devices (Sunnyvale, CA).

**Isolation and Culture of Primary Urothelial Cells.** We isolated and grew primary urothelial cells in culture as described previously (Teng et al., 2002). In brief, we obtained fresh human ureteral segments and placed them in supplemented Ham's F-12 nutrient medium (Sigma-Aldrich, St. Louis, MO) with 5% (v/v) fetal bovine serum, 5 $\mu$g/ml Apo-transferrin, 2.7 mg/ml glucose, 0.1 mM nonessential amino acids, 100 U/ml penicillin, 100 $\mu$g/ml streptomycin, and 2 mM L-glutamine (all from Sigma). The ureter was opened to expose the urothelium, and all fat and connective serosa were removed. The urothelial layer was manually removed, placed in fresh supplemented F-12 media, and minced. The tissue containing medium was transferred to a collagen-coated sterile tissue culture plate and grown in supplemented Ham's F-12 for 24 h. When cells achieved confluence, they were split by incubating with 0.25% Trypsin-EDTA (Sigma) for 10 min at 37°C. This high concentration of trypsin was used because the cells attached tightly to collagen. Ham's F-12 with 5% fetal bovine serum was added, and the lifted slurry was centrifuged at 500*g* for 5 min to collect the cells. Cells were grown in fresh Ham's F-12 nutrient medium until cells achieved confluence (passage 1). The cells were split again (using 0.05% trypsin); this cycle was repeated for a total of four passages. On the fifth splitting, cells were plated onto either collagen-coated stretch plates (57.75 $cm^2$/plate; FlexCell International, Hillsborough, NC) or collagen-coated Stage-Flexer membranes in 10-cm diameter Petri plates (FlexCell).

**Stretch-Induced Cytosolic Calcium Concentration ($[Ca^{2+}]_i$).** Primary urothelial cells were plated on Stage-Flexer membranes as described above and incubated in supplemented Ham's F-12 growth medium overnight to 50% confluence. The medium was replaced with Hank's minimal salt medium with calcium added to a final concentration of 1.5 mM. After 1-h incubation, 5 $\mu$M Fura-2 AM (methyl ester) was added, and cells were loaded for 30 min. The medium was then replaced with Hanks balanced salt solution (1.5 mM $Ca^{2+}$), and the cells were incubated at 37°C for 1 h to allow cleavage of the methyl ester and generation of free Fura-2 within the cytoplasm.

After Fura-2 loading, the membranes (containing attached urothelial cells at 50% confluence were removed from Petri plates and placed in the Stage-Flexer (Flexcell) apparatus for calcium imaging. Hanks' solution (100 $\mu$l ; 1.5 mM $Ca^{2+}$) was placed onto the cells, and the cells were covered with a glass coverslip. The Stage-Flexer was inverted to place the coverslip side nearest to the objective and fixed into place on the stage. Individual cells were identified on 20× objective such that 15 to 30 cells per field were visible. Fluorescence intensity was measured using intensified charge-coupled device dual excitation wavelengths of 340 and 380 nm. To maximize signal and diminish bleaching, a neutral density two-filter, 400-nm dichroic mirror and a 510-nm long-pass emission filter were in place during excitation (Checura and Parrish, 2006). Neutral absorbance was measured, and electronic images were taken every 5 s. After the resting images were taken, the cells were stretched using the Flexcell apparatus to 20% increase in cell surface size. A maximal 20% increase in surface area is equivalent to the increase in luminal surface area observed during intraluminal ureteral pressures of 46 mm Hg (Flexcell manual). Excitation and imaging were performed every 5 s for 5 min. After this time, stretch was removed, and excitation and imaging were continued at 5-s intervals for 1 min after returning the cells to the resting phase.

$[Ca^{2+}]_i$ at all time points was determined by the formula $[Ca^{2+}]_i = K_d\,[(R - R_{min})/(R_{max} - R)]\,[F^{380}{}_{max}/F^{380}{}_{min}]$, where $K_d$ is the binding affinity of Fura-2 to calcium, $R$ is the observed intensity value for each cell, $R_{min}$ is the 340:380 ratio in calcium-free medium, $R_{max}$ is 340:380 in 1 mM calcium, ($F^{380}{}_{max}/F^{380}{}_{min}$) is the emission at 510 nM in 1 mM $Ca^{2+}$ medium/$Ca^{2+}$-free medium. In our system, $Ratio_{min}$ = 0.48, $Ratio_{max}$ = 11, $K_d$ = 225, and $F^{380}{}_{max}/F^{380}{}_{min}$ = 10.

To test the repeatability and durability of the calcium response,

the above methodology was repeated three times, and $[Ca^{2+}]_i$ was measured and compared for each repeated stimulus. In addition, a separate subset of cells was stretched with 20% cyclic stretch (12 cycles per minute) for 1 h, and the above calcium concentration methodology was applied to the cells to determine the calcium response after 1 h of cyclic stretch.

**The Effect of Calcium Chelation on Stretch-Induced COX-2 Expression.** Primary urothelial cells were plated on six-well Bioflex (Flexcell) tissue culture plates as described above and incubated in supplemented Ham's F-12 growth medium overnight to 80 to 90% confluence. The cells were incubated with supplemented Ham's F-12 containing 0.3, 1, 3, 10, 30, or 100 $\mu$M BAPTA-AM or 0.1% DMSO (vehicle) for 30 min. The plates were placed on the cell stretch apparatus (FX-3000T; Flexcell), and Tension Plus software version 3.2 was used to control the apparatus. Tension (stretch) was applied to the bottom of the flexible stretch membranes by pressure-driven posts, controlled by the software. We stretched the cells to 20% increase in cell surface area using cyclic stretch at a rate of 12 cycles per min for 6 h, because this was determined previously to produce optimal induction of COX-2 expression (Jerde et al., 2006). Unstretched cells were used as controls.

After conclusion of the 6-h stretch period, protein collections were assayed for COX-2 and GAPDH protein by immunoblotting. Cells were collected in protease inhibitor containing lysis buffer (150 mM NaCl, 10 mM Tris, 1 mM EDTA, 1 mM phenylmethylsulfonyl fluoride, and 10 $\mu$g/ml each of leupeptin, aprotinin, and antipain; Sigma). Triton X-100 was added to a concentration of 1.0%, and the homogenate was incubated for 30 min at 4°C, followed by centrifugation for 10 min at 14,100*g*. The protein collections (20 $\mu$g/well) were resolved by electrophoresis in 10% SDS-polyacrylamide gel electrophoresis gel. Proteins were transferred to nitrocellulose blotting membranes, blocked overnight in blotto B + azide [10 g/l nonfat dry milk, 10 g/l bovine serum albumin, 0.5 g/l $NaN_3$ in 1× phosphate-buffered saline (PBS: 2.7 mM KCl, 1.5 mM $KH_2PO_4$, 136 mM NaCl, 8 mM $Na_2HPO_4$) + 0.05% (v/v) Tween 20], and incubated with either mouse monoclonal anti-COX-2 (18 h; Cayman Chemical, Ann Arbor, MI) or mouse monoclonal anti-GAPDH (1 h; Abcam, Poole, UK) diluted in blotto B + azide. After washing in PBS + 0.05% Tween 20, the blots were incubated with either goat anti-mouse or goat anti-rabbit IgGs conjugated to horseradish peroxidase for 1 h (Pierce, Rockford, IL) in blotto B (50 g/l nonfat dry milk, 20 g/l bovine serum albumin in PBS + 0.05% Tween 20). Peroxidase activity was detected via West Femto chemiluminescence reagent as directed by the manufacturer (Pierce). Photoimages were analyzed by Scion Image software (Scion Corp., Frederick, MD) for densitometry, and ratios of COX-2 to GAPDH were determined and compared between obstructed and normal ureter. Statistical evaluation was calculated with unpaired Student's *t* test (obstructed versus normal), and data are presented as mean (± S.D.) with corresponding *p* values.

To determine whether simple calcium induction would reciprocally induce COX-2 induction, we treated additional cells with 1 and 10 $\mu$M concentrations of 4-bromo-calcium ionophore for 6 h and measured COX-2 protein expression by immunoblotting in the presence and absence of cell stretch.

**Stretch-Induced Protein Kinase C Activation.** Primary urothelial cells were plated in six-well Bioflex collagen-coated tissue culture plates as described above and incubated in supplemented Ham's F-12 growth medium overnight to 80 to 90% confluence. To determine the presence of PKC isoforms, cells were stretched for 30, 45, 60, 90, or 120 min and immunoblotted for PKC $\alpha$, $\beta$1, $\beta$2, $\gamma$, $\delta$, $\varepsilon$, $\theta$, $\eta$, $\lambda/\iota$, and $\zeta$ isoforms. It was determined that human urothelial cells highly expressed PKC$\alpha$, $\beta$1, and $\zeta$, exhibited little expression of $\delta$, $\varepsilon$, $\eta$, and $\lambda/\iota$, and $\beta$2, $\gamma$, and $\theta$ were undetectable. It was also determined that PKC$\alpha$, $\beta$1, and $\zeta$ were down-regulated beyond 60 min of stretch. Based on these preliminary findings, we sought to determine the activation of PKC$\alpha$, $\beta$1, and $\zeta$ by measuring translocation to plasma membrane and nucleus after 45 min of stretch. For all experiments, unstretched cells and cells treated with 1 $\mu$M phorbol myristyl acetate (phorbol ester) were used as negative and positive controls, respectively.

To isolate the plasma membrane, we stretched four six-well plates (approximately $10^8$ cells) as described, washed once with PBS, and collected them in TEDK (10 mM Tris-HCl, pH 7.2, 0.3M KCl, 1 mM EDTA, 5 mM DTT, and 1× protease inhibitor cocktail) with a cell scraper. We homogenized the cells with 40 strokes of a Dounce homogenizer, centrifuged the suspension at 500*g* for 10 min to pellet the nuclei, and collected the supernatant. The supernatant was centrifuged at 27,000*g* for 30 min to collect membrane and organelles. The resulting pellet was resuspended in 2 ml of TEDK plus 15% sucrose and layered over a sucrose gradient of 30% sucrose in TEDK over 45%. The gradient was centrifuged at 76,000*g* for 3 h to separate the membrane fraction from the organelles. The 15 to 30% interface was collected in TEDK and centrifuged at 100,000*g* for 1 h. The pellet was resuspended in TEDK as the membrane fraction (Rivera-Bermúdez et al., 2002).

To isolate the cytosol, we stretched one six-well plate (approximately $10^7$ cells) as described, washed once with PBS, and collected them in TEDK with a cell scraper. We homogenized the cells with 40 strokes of a Dounce homogenizer, centrifuged the suspension at 500*g* for 10 min to pellet the nuclei, and collected the supernatant. The plasma membrane and nuclei were pelleted by centrifugation at 100,000*g* for 1 h. The supernatant was collected as the cytosolic fraction (Rivera-Bermúdez et al., 2002).

To isolate the nuclei, we stretched three six-well plates (approximately $5 \times 10^7$ cells) as described, washed once with buffer A (10 mM Tris base, pH 7.8, 5 mM $MgCl_2$, 10 mM KCl, 0.3 mM EGTA, 0.3 mM sucrose, 10 mM $\beta$-glycerophosphate, 1 mM phenylmethylsulfonyl fluoride, 0.5 mM DTT, and 1% protease inhibitor cocktail), and collected them in buffer A with a cell scraper. After placing the cells on ice for 15 min, the cells were lysed with Nonidet P-40 at a final concentration of 0.6% and underwent vortexing for 20 s at the highest speed. The suspension was centrifuged at 7200*g* for 2 min to pellet the nuclei, and the pellet was resuspended in 300 $\mu$l of buffer (20 mM Tris base, pH = 7.8, 5 mM $MgCl_2$, 320 mM KCl, 0.5 mM DTT, and 1% protease inhibitor cocktail). This suspension was incubated on ice for 15 min to disrupt the nuclei and solubilize the proteins. The suspension was centrifuged at 13,500*g* for 15 min, and the supernatant was collected as the nuclear extract (Rivera-Bermúdez et al., 2002).

Protein extracts from all three fractions were quantified and immunoblotted for PKC isoforms $\alpha$, $\beta$1, and $\zeta$. Fraction purity for cytosolic and nuclear protein extraction was assessed by immunoblotting each fraction for lactate dehydrogenase (exclusively cytosolic protein) and nuclear lamin B1 (exclusively nuclear protein) using the immunoblotting methods described. Plasma membrane fraction purity was assessed by assaying each fraction for adenylyl cyclase activity (exclusively plasma membrane protein) using an activity assay (Molecular Devices) in which protein extract from each fraction was assessed for its ability to generate cAMP from ATP in conditions recommended by the manufacturer.

**The Effect of Protein Kinase C Inhibition on Stretch-Induced COX-2 Expression.** Primary urothelial cells were plated on six-well Bioflex tissue culture plates as described above and incubated in supplemented Ham's F-12 growth medium overnight to 80 to 90% confluence. The cells were incubated with supplemented Ham's F-12 containing 1, 10, or 100 nM bisindolylmaleimide-1; 3, 10, or 30 $\mu$M myristoylated PKC pseudosubstrate peptide; or 0.1% DMSO (vehicle) for 1 at a rate of 12 cycles/min for 6 h, as described previously. Unstretched cells were used as controls. After the conclusion of the 6-h stretch period, protein collections were assayed for COX-2 and GAPDH protein by immunoblotting.

Additional primary urothelial cells were plated on six-well Bioflex tissue culture plates as described above and incubated in supplemented Ham's F-12 growth medium overnight to approximately 60% confluence. Oligofectamine-siRNA complexes were generated for 30 min in OPTI-MEM medium in conditions recommended by the man-

ufacturer (Invitrogen, Carlsbad, CA) using 23 base siRNA sequences (Dharmacon, Lafayette, CO) directed against PKCα, PKCβ1, or PKCζ. The complexes were added to the cells in supplemented Ham's F-12 such that the final dilution in the wells was 10 μl of Oligofectamine per milliliter of medium and either 250 nM PKCα, 500 nM PKCβ1, or 500 nM PKCζ siRNA. These were the transfection conditions determined to be optimal in preliminary experiments. The transfections were allowed to progress for 48 h; this time point was determined to be optimal in preliminary experiments. Additional cells were transfected with negative control RNA shown previously to not silence any gene in the human genome (Dharmacon), and untransfected cells were used as a second negative control. After the 48-h transfection period, the cells were harvested, and protein extracts were immunoblotted for GAPDH, COX-2, PKCα, PKCβ1, and PKCζ, as described above. PKC expression knockdown was determined by measuring densitometry of each PKC band relative to its GAPDH loading control and compare this to cells transfected with negative control RNA.

**siRNA Controls.** To determine the effect of siRNA transfection and reagents on COX-2 and PKC expression in urothelial cells, preliminary experiments were performed in which stretched and unstretched urothelial cells were transfected with unrelated siRNA controls with Oligofectamine, treated with Oligofectamine alone, or untreated. No effect of nonsense siRNA transfection or Oligofectamine was observed, and inducibility of COX-2 was unaffected.

**Calcium-Dependence of PKCζ Activation.** To examine the inter-relationship of the critical PKC isoform and calcium in stretch-induced COX-2 induction, we sought to determine whether PKCζ activation was dependent on calcium. First, activation of the ζ isoform of PKC was determined by phosphorylation of threonine residues 403 and 410 by phosphospecific antibody (Abcam). Cells were stretched for 0.5, 1, 2, and 4 h with 20% cyclic stretch (12 cycles/min), total cell protein extract was collected, and phosphorylation of PKCζ was determined by immunoblotting. After confirming that optimal induction occurred within 2 h of stretch, cells were incubated with supplemented Ham's F-12 containing 3, 10, or 30 μM BAPTA-AM or 0.1% DMSO (vehicle) for 30 min. Cells were stretched for 1 h with 20% cyclic stretch (12 cycles/min), and total cell protein extract was collected in the presence of protease and phosphatase inhibitors. Immunoblotting for phospho-(Thr 403/410) PKCζ activation was determined by immunoblotting by phosphospecific antibody.

## Results

**The Effect of Stretch on $[Ca^{2+}]_i$.** Figure 1, A through D, show individual cell fields after various times of stretch applied to resting cells (A) with the color intensity relating to changes in $[Ca^{2+}]_i$ such that the range of blue to white represents low to high levels. The average values of multiple individual cell fields ($n = 5$) of $[Ca^{2+}]_i$ is represented in Fig. 1F and demonstrates that $[Ca^{2+}]_i$ increased from 44 nM in resting cells to 430 nM after 30 s of 20% stretch. After 60 s of stretch, $[Ca^{2+}]_i$ began to gradually decrease throughout the 5-min stretch period to an average of 210 nM. All measured differences in cells stretched to 20 and 10% were statistically significant above unstretched controls at all time points of stretching, as determined by unpaired Student's $t$ test ($p$ values $<0.01$). In addition, 20% stretch produced statistically significant increase compared with 10% stretch after 15 s of stretch, continuing throughout the stretch. Upon removing stretch from the cells, a second transient increase in $[Ca^{2+}]_i$ occurred, to a maximal point of 405 nM. This second increase lasted approximately 10 s before a rapid decrease that reduced $[Ca^{2+}]_i$ to an average of 62 nM. No statistical difference was noted in calcium induction induced by removing 20% stretch and 10% stretch. The rapid induction of $[Ca^{2+}]_i$ was repeatable within each experiment, because the cells could be induced to concentrations of $[Ca^{2+}]_i$ greater than 400 nM at least three times in succession. Likewise, cells stretched for 1 h before calcium measurements had responsiveness similar to previously unstretched cells, because all cells were inducible to greater than 400 nM $[Ca^{2+}]_i$. Positive control cells treated with 10 μM 4-bromo-calcium ionophore exhibited $[Ca^{2+}]_i$ of 962 nM after 60 s of treatment.

**The Effect of Calcium Chelation on Stretch-Induced COX-2 Expression.** Stretch induced an 8-fold increase in COX-2 protein content compared with nonstretched controls (the ratio of COX-2 to GAPDH was 1.26 (± 0.15) in stretched cells and 0.16 (± 0.04) in control cells ($n = 6$, $p = 0.001$) (Fig.

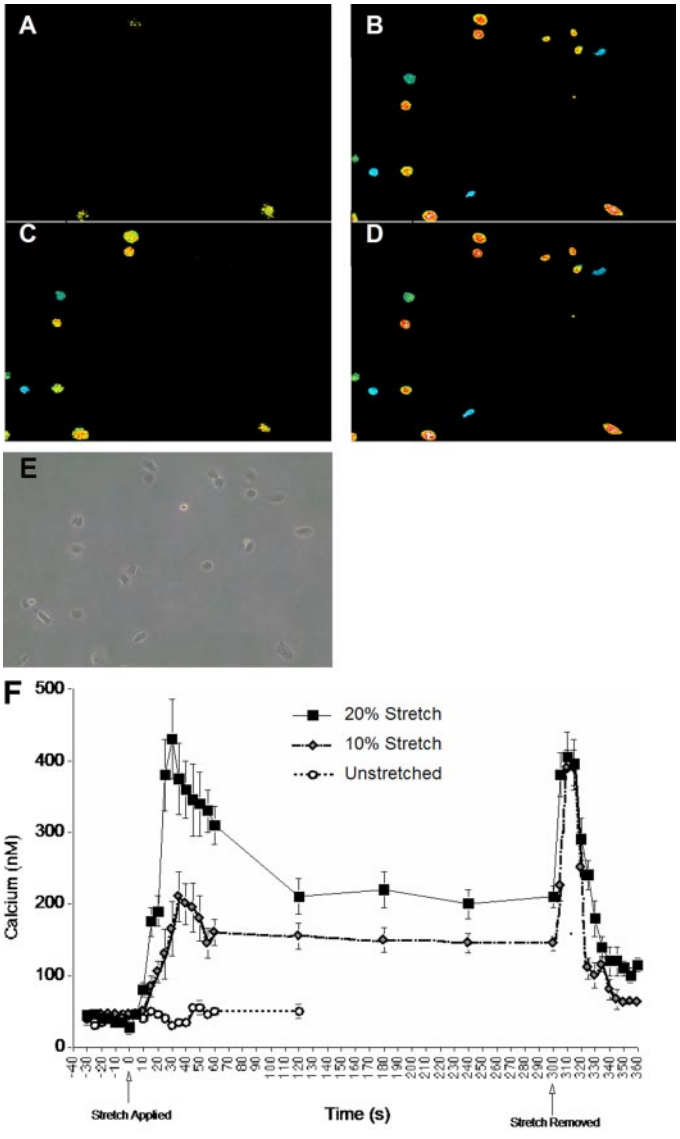


**Fig. 1.** Fura-2 ratio ($A_{340}/A_{380}$) in primary urothelial cells. A, one cell field of unstretched cells before the experiment. B, cells stretched for 40 s. C, cells stretched for 300 s. After stretch was released (D), a second spike in $[Ca^{2+}]_i$ occurred. E, a light-field micrograph of the cells stretched to generate the color images in A to D. F, the average $[Ca^{2+}]_i$ in stretched urothelial cells as determined by eq. 1, 15 determinations per data point, $n = 5$ total cell lines. Maximal induction of calcium was observed at 30 s of stretch, after which time $[Ca^{2+}]_i$ gradually decreased. Upon release of stretch, a transient spike in $[Ca^{2+}]_i$ occurred. The average basal $[Ca^{2+}]_i$ was 44 nM, whereas maximal $[Ca^{2+}]_i$ (962 nM) was obtained with 10 μM calcium ionophore.

2A). Calcium chelation with BAPTA-AM reduced this induction in a dose manner such that the ratio of COX-2 to GAPDH was 0.54 in 1 $\mu$M BAPTA-AM-treated stretched cells, 0.15 in 3 $\mu$M BAPTA-AM-treated stretched cells, 0.06 in 30 $\mu$M BAPTA-AM-treated stretched cells, and 0.07 in 100 $\mu$M BAPTA-AM-treated cells. All four concentrations studied produced statistical significance relative to vehicle (DMSO)-treated control cells (Student's $t$ test, $p < 0.01$). The highest concentration of calcium chelation also reduced the expression of COX-2 in unstretched cells, because the ratio of COX-2 to GAPDH was reduced from 0.16 in untreated unstretched cells to 0.06 with 100 $\mu$M BAPTA-AM treatment. This was the only concentration of BAPTA-AM to exhibit significant inhibition in unstretched cells ($p = 0.02$).

To determine whether induction of calcium flux alone was sufficient to induce COX-2 expression, we treated stretched and unstretched cells with 4-bromo-calcium ionophore for 6 h. Induction of calcium flux with 1 $\mu$M ionophore induces COX-2 expression 8-fold in unstretched cells (Fig. 2B). The addition of 10 $\mu$M ionophore had only a marginal increase greater than 1 $\mu$M. The addition of ionophore to stretched cells doubled the expression of COX-2; however, this induction was equal to that of ionophore alone, suggesting that calcium flux and stretch induce COX-2 via a similar mechanism.

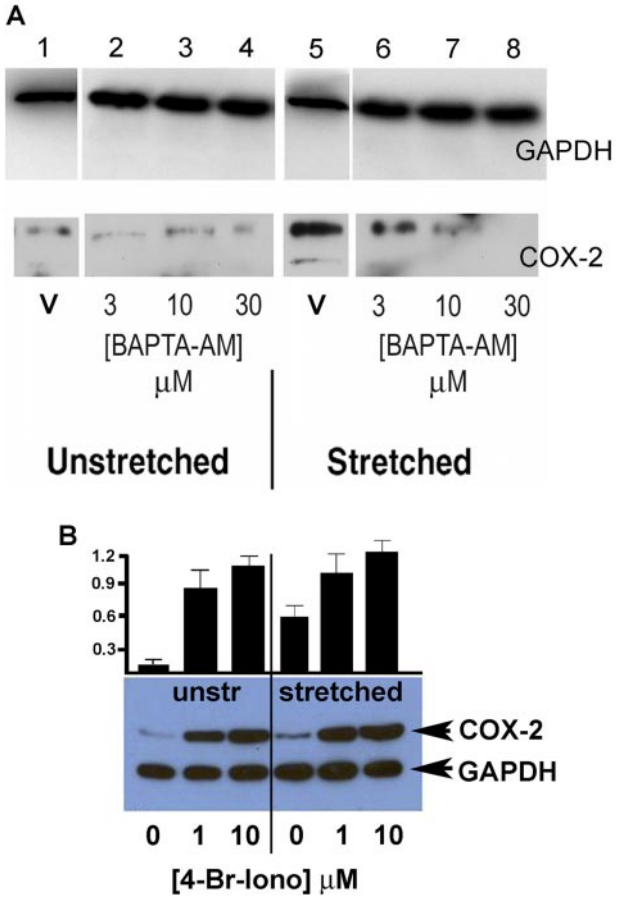


**Fig. 2.** Calcium chelation attenuates stretch-induced COX-2 expression, and induction of calcium flux is sufficient to induce COX-2. Stretch induced an 8-fold increase in COX-2 protein levels in vehicle (V)-treated tissues compared with nonstretched controls. Calcium chelation with BAPTA-AM dose-dependently eliminated this induction (A; $n = 5$). B, induction of calcium flux with 4-bromo-calcium ionophore induces COX-2 expression dose-dependently (1 and 10 $\mu$M) in stretched and unstretched urothelial cells. Data in the graph are the ratio of COX-2 expression to GAPDH, the average of three cell lines ($n = 3$) performed in duplicate (*, $p < 0.05$, ionophore versus vehicle).

**The Effect of Stretch on PKC Translocation.** In preliminary experiments, we determined that stretched and unstretched human urothelial cells expressed PKC $\alpha$, $\beta$1, and $\zeta$ isoforms. No presence of $\beta$2, $\gamma$, $\eta$, and $\theta$ were observed and only weak presence of $\delta$, $\varepsilon$, and $\lambda/\iota$ were identified (data not shown). Stretched cells exhibited marked translocation of PKC $\alpha$, $\beta$1, and $\zeta$ to the plasma membrane and nucleus, indicating activation (Fig. 3). For PKC$\alpha$, urothelial cells stretched for 45 min exhibited a plasma membrane to cytosol (m/c) ratio of 2.7 and a nucleus to cytosol (n/c) ratio of 3.1 compared with a m/c ratio of 0.16 ($p = 0.007$) and a n/c ratio of 0.13 ($p = 0.03$) in unstretched cells ($n = 4$). For PKC$\beta$1, stretched cells exhibited an m/c ratio of 6.9 and an n/c ratio of 6.3 compared with an m/c ratio of 0.07 ($p = 0.02$) and an n/c ratio of 0.06 ($p = 0.002$) in unstretched cells ($n = 4$). For PKC$\zeta$, stretched cells exhibited an m/c ratio of 8.8 and a n/c ratio of 9.0 compared with an m/c ratio of 1.1 ($p = 0.04$) and an n/c ratio of 1.1 ($p = 0.02$) in nonstretched cells ($n = 4$). Phorbol ester induced translocation of PKC$\alpha$ (m/c: $p = 0.02$; n/c: $p = 0.03$) and $\beta$1 (m/c: $p = 0.01$; n/c: $p = 0.003$) but not $\zeta$ (m/c: $p = 0.80$; n/c: $p = 0.85$). We verified cell fraction purity by blotting for lactate dehydrogenase (a cytosolic protein) and nuclear lamin B1 (a nuclear protein) and assessing adenylyl cyclase activity (plasma membrane protein). These data indicate that PKC is activated and translocated to the plasma membrane and nuclear region during cell stretch.

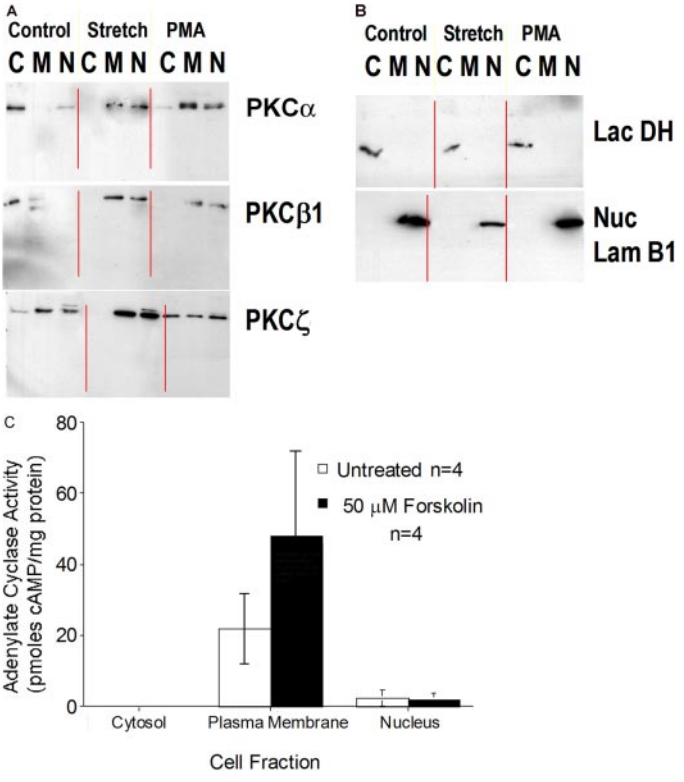


**Fig. 3.** A, blotting for PKC isoforms in cytosol (C), nucleus (N), and membrane (M) with polyclonal antibodies. B, fraction purity was verified by blotting for lactate dehydrogenase and nuclear lamin B1. C, plasma membrane fraction purity was verified by assessment of adenylyl cyclase activity. These data indicate that fractions were pure enough for assessment of PKC translocation.

**The Effect of Pharmacological PKC Inhibition on Stretch-Induced COX-2 Expression.** In untreated cells, the ratio of COX-2 to GAPDH was 1.20 in stretched cells and 0.12 ($n = 6$, $p = 0.001$) in control cells (Fig.s 4 and 5). Pharmacological PKC inhibition with bisindolylmaleimide-1 reduced COX-2 induction in a concentration-dependent manner. COX-2-to-GAPDH ratios were 0.92, 0.22 ($p = 0.001$), and 0.13 ($p = 0.005$) in 1, 10, and 100 nM bisindolylmaleimide-1-treated stretched cells, respectively ($n = 6$; Fig. 4). Likewise, COX-2 to GAPDH ratios were 0.80, 0.32 ($p = 0.006$), and 0.30 ($p = 0.01$) in 3, 10, and 30 $\mu$M PKC pseudosubstrate peptide-treated stretch-induced cells, respectively (Fig. 5). Neither PKC inhibitor reduced COX-2 expression significantly from untreated controls in unstretched cells.

**The Effect of PKCα, β1, and ζ RNA Interference on Stretch-Induced COX-2 Expression.** Transfection of urothelial cells with siRNA directed against PKCα reduced PKCα expression by 91%. In these cells, the COX-2-to-GAPDH ratio was slightly reduced from 1.0 in stretched control siRNA transfected cells to 0.79 in PKCα RNAi transfectants (Fig. 6). However, this reduction was not statistically significant, although a clear trend was present ($p = 0.06$, $n = 4$). Transfection of cells with siRNA directed against PKCβ1 reduced PKCβ1 expression by 60%. This had no significant effect on stretch-induced COX-2 expression. However, unstretched cells transfected with siRNA directed against PKCβ1 exhibited a slight, statistically insignificant trend of increased COX-2 expression compared with non-transfected unstretched controls ($n = 4$, $p = 0.08$) (Fig. 6). Transfection of urothelial cells with siRNA directed against PKCζ inhibited PKCζ expression by 71%. The COX-2-to-GAPDH ratio was significantly reduced from 1.0 in stretched siRNA control cells to 0.32 in PKCζ RNAi transfectants ($p = 0.005$, $n = 4$) (Fig. 6).

**Calcium Dependence of PKCζ Activation.** To determine the dependence of PKCζ induction on calcium signaling, we pretreated urothelial cells with BAPTA-AM for 30 min before stretching. We then analyzed cellular protein for PKCζ phosphorylation (a marker of PKCζ activation) by immunoblotting with phosphospecific antibodies. Stretch of urothelial cells for 2 h induced the phosphorylation of PKCζ 3-fold, indicating activation (Fig. 7). Chelation of intracytosolic calcium with BAPTA attenuated this response, because 30 $\mu$M BAPTA-AM reduced $PO_4$-PKCζ to unstretched levels.

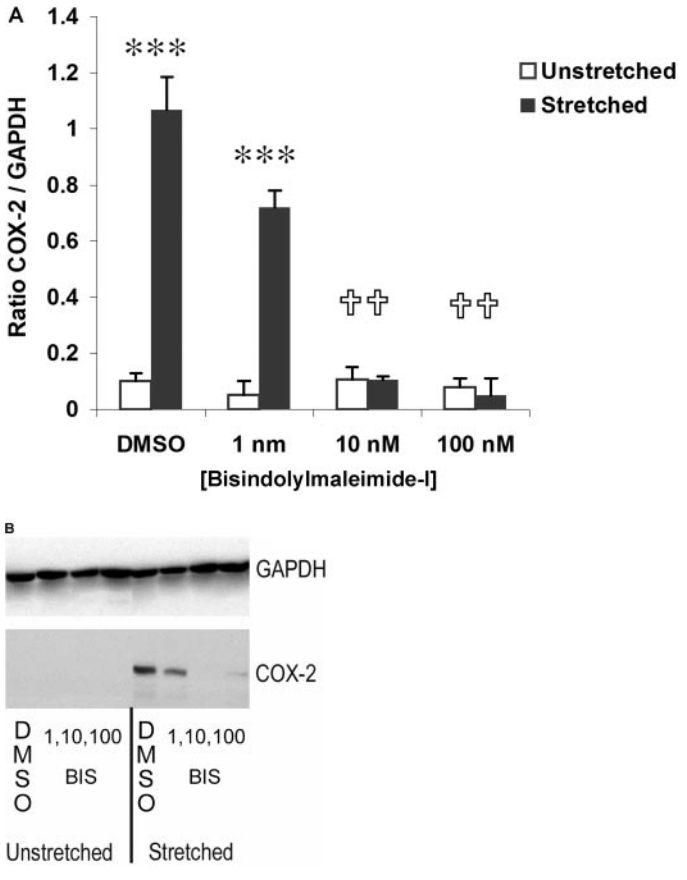


**Fig. 4.** Pharmacological PKC inhibition attenuates stretch-induced COX-2 expression. A, cell stretch induced COX-2 expression (***$p <$ 0.001- stretched versus unstretched cells) as shown by quantified data illustrating concentration-dependent attenuation. Bisindolylmaleimide (Bis; 10 nM) produced statistically significant attenuation (††, $p < 0.01$ stretched cells: Bis versus DMSO vehicle, $n = 6$) of stretch-induced COX-2 expression. B, immunoblot illustrating bisindolylmaleimide-attenuation of stretch-induced COX-2 expression.

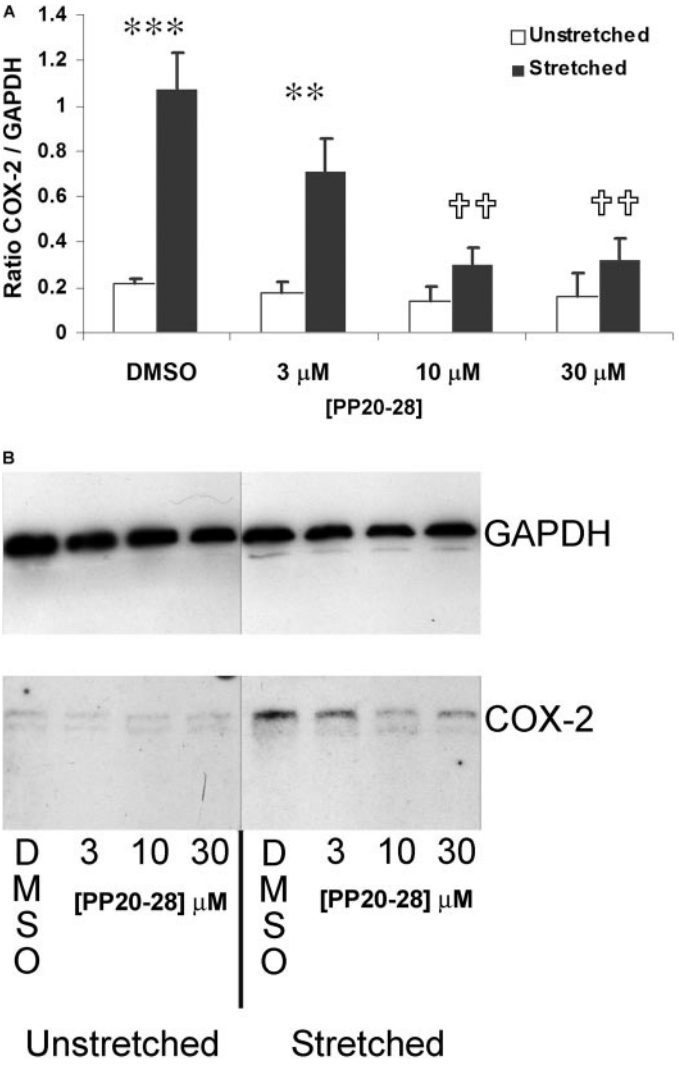


**Fig. 5.** Pseudosubstrate PKC inhibition attenuates stretch-induced COX-2 expression. A, 10 $\mu$M pseudosubstrate peptide 20-28 (PP 20-28) inhibitor produced statistically significant attenuation of stretch-induced COX-2 expression relative to vehicle-treated cells (DMSO), as illustrated by quantified data from immunoblots (††, $p < 0.01$ stretched cells: PP 20-28 versus DMSO vehicle, $n = 4$). B, immunoblot illustrating the effect of PP 20-28 inhibitor on stretch-induced COX-2 expression.

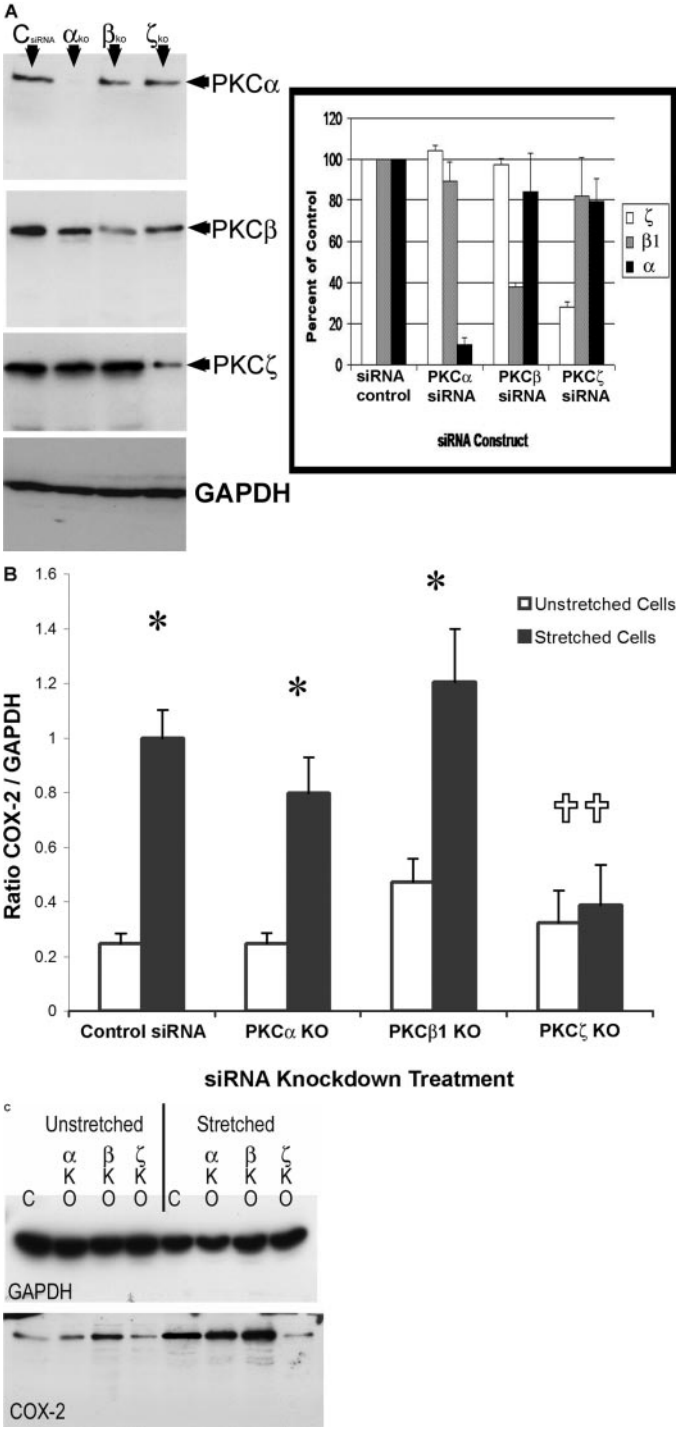


**Fig. 6.** siRNA-PKC$\zeta$ transfection attenuates stretch-induced COX-2 expression. A, immunoblots demonstrating PKC isoform specific expression knockdown by specific PKC siRNAs. Expression of PKC$\alpha$, $\beta$1, and $\zeta$ in control (nontransfected) cells was compared with that in PKC$\alpha$, $\beta$1, and $\zeta$ siRNA transfected cells. B, quantified data demonstrates PKC$\zeta$-siRNA attenuated COX-2 induction. Stretch of cells transfected with control siRNAs or siRNA directed against PKC$\alpha$ or PKC$\beta$ significantly induced COX-2 expression (*, $p < 0.05$ stretched versus unstretched control siRNA-treated cells, $n = 4$). However, cells transfected with siRNA against PKC$\zeta$ showed significant attenuation of stretch-induced COX-2 expression (††, $p = 0.005$, PKC$\zeta$ siRNA-transfected cells versus control siRNA-transfected cells, $n = 4$). PKC$\alpha$ siRNA may have a modulatory effect, although this effect is statistically insignificant with these data sets ($p = 0.21$, $n = 4$). C, immunoblot illustrating PKC$\zeta$ siRNA attenuation of stretch-induced COX-2 expression.

The data shown are the ratio of $PO_4$-PKC$\zeta$ to GAPDH quantified from three cell lines ($n = 3$) in duplicate. Total PKC$\zeta$ levels did not change in this experiment, indicating that phosphorylation and activation processes are involved in $PO_4$-PKC$\zeta$ increase rather than induction of PKC$\zeta$ expression.

## Discussion

Our data indicate that calcium and PKC$\alpha$, $\beta$1, and $\zeta$ are induced by cell stretch in primary human urothelial cells. In addition, our data indicate that calcium and PKC$\zeta$ are necessary for COX-2 expression in this model and suggest that PKC$\alpha$ may play a secondary role. This is the first report specifically linking PKC$\zeta$ to mechanically induced COX-2 expression. Although other studies have used pharmacological inhibitors to determine that PKC isoforms are involved in mechanotransduction involving vascular endothelial cells and bone cells, this is the first study that we are aware of that uses siRNA targeting to specifically silence expression of the PKC$\zeta$ isoform. This is also the first report to illustrate specific PKC isoform activation in response to cell stretch. Although PKC$\zeta$ has been implicated in COX-2 induction in overexpression studies (Miller et al., 1997), this is the first report identifying calcium and PKC as being integral to stretch-induced COX-2 expression in urothelial cells, the primary prostaglandin producing cells in the urinary tract, particularly as it relates to the pathophysiology of ureteral obstruction (Ali et al., 1998).

Our previous work illustrates the reproducibility and reliability of the urothelial cell model in relation to in vitro ureteral obstruction. In addition, Park and associates (1997) have demonstrated similar reproducibility using a bladder smooth muscle cell model and in vivo distended detrusor. Still, the calcium flux associated with rapidly inducible cell stretch produced in vitro may not correlate temporally or quantitatively with what is actually occurring in vivo. Our cell culture model has shown a more rapid induction of gene expression than what is observed in our in vivo obstruction model. Likewise, it is possible that differential PKC expression in vitro could distort the overall importance of each PKC isoform as it relates to their contribution to in vivo mechano-

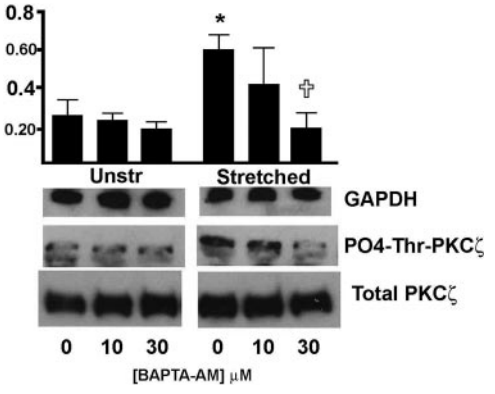


**Fig. 7.** Stretch-induced PKC$\zeta$ is dependent on calcium. Stretch of urothelial cells induced the phosphorylation of PKC$\zeta$ 3-fold, indicating activation (*, $p < 0.05$) (stretched versus unstretched, $n = 3$). Chelation of intracytosolic calcium with BAPTA attenuated this response, because 30 $\mu$M BAPTA-AM reduced $PO_4$-PKC$\zeta$ to unstretched levels [†, $p < 0.05$ (0 versus 30 $\mu$M BAPTA-AM), $n = 3$]. The data shown are the ratio of $PO_4$-PKC$\zeta$ to GAPDH quantified from three cell lines ($n = 3$) in duplicate.

transduction in general and distension-induced COX-2 expression in particular. New isoform-selective PKC inhibitors are in development, and inducible gene knockout animal models may allow for the assessment of selective isoform inhibition in vivo.

We did not expect PKCζ to be the primary isoform of PKC involved in stretch-induced COX-2 expression, and it was even more unexpected that PKCα would have such a minimal effect. Our data clearly show the dependence of COX-2 induction on calcium, yet PKCζ is a calcium-independent isoform of PKC. Our data show that PKCζ activation, as measured by phosphorylation, is dependent on available calcium in our system. However, the questions of how and to what extent PKCζ might be dependent on calcium in cell biology are unresolved by our study and were not the intent of our study. This effect could be direct or indirect, and future work will be directed at answering these important questions. Although little is known regarding PKCζ activation, there is evidence that phosphoinositide-dependent kinase-1 phosphorylates and activates PKCζ secondary to phosphoinositol triphosphate kinase signaling. (Hirai and Chida, 2003) Recent evidence from bone cells indicates that this is a calcium-driven process (Danciu et al., 2003), but the role calcium plays in this process is not clear. It is feasible that the role of calcium in phosphoinositide-dependent kinase-1 activation and the role of the calcium and classic PKC isoforms in our model are related, and some level of cross-talk between the classic and atypical PKC isoforms may occur during urothelial cell stretch. Classic PKC isoforms and PKCζ have been shown to cross-talk in NIH3T3 cells induced with phorbol ester (Kim et al., 1997). Although we found no effect of PKCβ1 knockdown on stretch-induced COX-2 expression, PKCβ1 may compensate for the lack of PKCα activity the presence of PKCα knockdown. Future studies should be directed toward evaluating these hypotheses with COX-2 expression and PKCζ activation studies in the presence of calcium chelation, PKCα/PKCβ1 double knockouts, and phosphoinositol-3 kinase inhibitors. Finally, although siRNA knockdown of whole-cell PKCα or β1 protein gives inconclusive results, these data do not yet consider any differences in nuclear or plasma membrane localization of these isoforms. It is possible that, even with 91 and 62% knockdown of PKCα and β1, respectively, there still could be a significant concentration of activated kinase in the nuclear or plasma membrane. Studies evaluating the cellular localization of the PKC isoforms during RNA interference should be performed.

Calcium and PKC may induce COX-2 in response to cell stretch via several known pathways. Many signaling cascades of COX-2 induction have been identified, including those involving mitogen-activated protein kinases, phosphoinositol-3 kinase-Akt, nuclear factor κB, steroid hormone receptors, and extracellular matrix proteins, all of which may be modulated by calcium and PKC (Appleby et al., 1994; Yamamoto et al., 1995; Santen et al., 2002; Tamura et al., 2002; Di Mari et al., 2003). However, most of these studies involved hormone or mitogen-induced conditions, and data investigating mechanosensing pathways of COX-2 induction remain sparse. Stretch-induced COX-2 expression in bladder smooth muscle, renal podocytes, and osteoblasts does seem to be mitogen-activated protein kinase-dependent, especially with regard to p38 (Naruse et al., 2003; Fitzgerald et al., 2004; Martineau et al., 2004). In addition, deletion analysis of COX-2 promoter elements has determined the importance of CCAAT/enhancer-binding protein-β, cAMP response element, and activator protein-1 elements in shear stress-induced COX-2 expression in murine osteoblasts (Ogasawara et al., 2001). However, the triggering cascades of these molecules are yet to be determined in mechanically stimulated cells. The cellular mechanisms by which stretch induces COX-2 expression are an active area of investigation, and will probably lead to pharmacological targets of intervention for stretch and pressure-related diseases.

**Acknowledgments**

We gratefully acknowledge Dr. Abdullah Kaya for expert assistance in operating the fluorescent imaging microscope, Dr. Glen Leverson for statistical analysis of the data, Dr. Paul Bertics for insightful discussions of the data, and Nicholas Weber for imaging analysis and manuscript preparation.

**References**

Ali M, Angelo-Khattar M, Thulesius L, Fareed A, and Thulesius O (1998) Urothelial synthesis of prostanoids in the ovine ureter. *Urol Res* **26:**171–174.
Appleby SB, Ristimaki A, Neilson K, Narko K, and Hla T (1994) Structure of the human cyclo-oxygenase-2 gene. *Biochem J* **302:**723–727.
Baçsar I, Bircan K, Tasar C, Ergen A, Cakmak F, and Remzi D (1991) Diclofenac sodium and spasmolytic drugs in the treatment of ureteral colic: a comparative study. *Int Urol Nephrol* **23:**227–230.
Brune K and Neubert A (2001) Pharmacokinetic and pharmacodynamic aspects of the ideal COX-2 inhibitor: a pharmacologist's perspective. *Clin Exp Rheumatol* **19:**S51–S57.
Checura CM and Parrish JJ (2006) The role of calcium in maturation and activation of horse oocytes. *Anim Reprod Sci* **94:**340–342.
Chou SY, Cai H, Pai D, Mansour M, and Huynh P (2003) Regional expression of cyclooxygenase isoforms in the rat kidney in complete unilateral ureteral obstruction. *J Urol* **170:**1403–1408.
Clark JY, Thompson IM, and Optenberg SA (1995) Economic impact of urolithiasis in the United States. *J Urol* **154:**2020–2024.
Cole RS, Fry CH, and Shuttleworth KE (1988) The action of the prostaglandins on isolated human ureteric smooth muscle. *Br J Urol* **61:**19–26.
Colletti AE, Vogl HW, Rahe T, and Zambraski EJ (1999) Effects of acetaminophen and ibuprofen on renal function in anesthetized normal and sodium-depleted dogs. *J Appl Physiol* **86:**592–597.
Danciu TE, Adam RM, Naruse K, Freeman MR, and Hauschka PV (2003) Calcium Regulates the PI3K-Akt pathway in stretched osteoblasts. *FEBS Lett* **536:**193–197.
Di Mari JF, Mifflin RC, Adegboyega PA, Saada JI, and Powell DW (2003) IL-1α-induced COX-2 expression in human intestinal myofibroblasts is dependent on a PKCζ-ROS pathway. *Gastroenterology* **124:**1855–1865.
Fitzgerald JB, Jin M, Dean D, Wood DJ, Zheng MH, and Grodzinsky AJ (2004) Mechanical compression of cartilage explants induces multiple time-dependent gene expression patterns and involves intracellular calcium and cyclic AMP. *J Biol Chem* **279:**19502–19511.
Foegh ML, Hecker M, and Ramwell PW (1999) The eicosanoids: prostaglandins, thromboxanes, leukotrienes and related compounds, in *Basic and Clinical Pharmacology* (Katzung BG ed) pp 311–325, McGraw-Hill, New York.
Gulmi FA, Felson D, and Vaughan ED (1998) Physiology of ureteral obstruction, in *Campbell's Urology* (Walsh PC, Retik AB, Vaughan ED, Wein A eds) pp 324–379, WB Saunders, Philadelphia.
Hamill OP and Martinac B (2001) Molecular basis of mechanotransduction in living cells. *Physiol Rev* **81:**685–740.
Hernández J, Astudillo H, and Escalante B (2002) Angiotensin II stimulates cyclooxygenase-2 mRNA expression in renal tissue from rats with kidney failure. *Am J Physiol Renal Physiol* **282:**F592–F598.
Hirai T and Chida K (2003) Protein kinase C zeta (PKC zeta): activation mechanisms and cellular functions. *J Biochem* **133:**1–7.
Inoue H, Taba Y, Miwa Y, Yokota C, Miyagi M, and Sasaguri T (2002) Transcriptional and posttranscriptional regulation of cyclooxygenase-2 expression by fluid shear stress in vascular endothelial cells. *Arterioscler Thromb Vasc Biol* **22:**1415–1420.
Jerde TJ, Mellon WS, Bjorling DE, and Nakada SY (2006) Evaluation of urothelial stretch-induced cyclooxygenase-2 expression in novel human cell culture and porcine in vivo ureteral obstruction models. *J Pharmacol Exp Ther* **317:**965–972.
Kim SJ, Chang YY, Kang SS, and Chun SJ (1997) Phorbol ester effects in atypical protein kinase C ζ overexpressing NIH3T3 cells: possible evidence for crosstalk between protein kinase C isoforms. *Biochem Biophys Res Commun* **237:**336–339.
Kujubu DA, Fletcher BS, Varnum BC, Lim RW, and Herschmann HR (1991) TIS10, a phorbol ester tumor-promoter-inducible mRNA from Swiss 3T3 cells, encodes a novel prostaglandin synthase/cyclooxygenase homologue. *J Biol Chem* **266:**12866–12872.
Lanza GL, Rack MF, Simon TJ, Quan H, Bolognese JA, Hoover ME, Wilson FR, and Harper SE (1999) Specific inhibition of cyclooxygenase-2 with MK-0966 is associated with less gastroduodenal damage than either aspirin or ibuprofen. *Aliment Pharmacol Ther* **13:**761–767.

Malhotra A, Kang BP, Opawumi D, Belizaire W, and Meggs LG (2001) Molecular biology of protein kinase C signaling in cardiac myocytes. *Mol Cell Biochem* **225:**97–107.
Martineau LC, McVeigh LI, Jasmin BJ, and Kennedy CR (2004) p38 MAP kinase mediates mechanically induced COX-2 and PG EP4 receptor expression in podocytes: implications for the actin cytoskeleton. *Am J Physiol Renal Physiol* **286:** F693–F701.
Miller BW, Baier LD, and Morrison AR (1997) Overexpression of protein kinase C-zeta isoform increases cyclooxygenase-2 and inducible nitric oxide synthase. *Am J Physiol* **273:**C130–C136.
Mukherjee D, Nissen SE, and Topol EJ (2001) Risk of cardiovascular events associated with selective COX-2 inhibitors. *JAMA* **286:**954–959.
Nakada SY, Jerde TJ, Jacobson LM, Saban R, Bjorling DE, and Hullett DA (2002) Cyclooxygenase-2 expression is upregulated in obstructed human ureter. *J Urol* **168:**1226–1229.
Naruse K, Miyauchi A, Itoman M, and Mikuni-Takagaki Y (2003) Distinct anabolic response of osteoblast to low-intensity pulsed ultrasound. *J Bone Miner Res* **18:**360–369.
Newton AC (1995) Protein kinase C: structure, function, and regulation. *J Biol Chem* **270:**28495–28498.
Ogasawara A, Arakawa T, Kaneda T, Takuma T, Sato T, Kaneko H, Kumegawa M, and Hakeda Y (2001) Fluid shear stress-induced cyclooxygenase-2 expression is mediated by C/EBP beta, cAMP-response element-binding protein, and AP-1 in osteoblastic MC3T3–E1 cells. *J Biol Chem* **276:**7048–7054.
Oren R and Ligumsky M (1994) Indomethacin-induced colonic ulceration and bleeding. *Ann Pharmacother* **28:**883–885.
Park JM, Yang T, Arend LJ, Smart AM, Schnermann JB, and Briggs JP (1997) Cyclooxygenase-2 is expressed in bladder during fetal development and stimulated by outlet obstruction. *Am J Physiol* **273:**F538–F544.
Ramello A, Vitale C, and Marangella M (2000) Epidemiology of nephrolithiasis. *J Nephrol* **13 (Suppl 3):**S45–S50.
Rivera-Bermúdez MA, Bertics PJ, Albrecht RM, Mosavin R, and Mellon WS (2002) 1,25-Dihydroxyvitamin D3 selectively translocates PKCalpha to nuclei in ROS 17/2.8 cells. *Mol Cell Endocrinol* **188:**227–239.
Santen RJ, Song RX, McPherson R, Kumar R, Adam L, Jeng MH, and Yue W (2002) The role of mitogen-activated protein (MAP) kinase in breast cancer. *J Steroid Biochem Mol Biol* **80:**239–256.
Tamura M, Sebastian S, Gurates B, Yang S, Fang Z, and Bulun SE (2002) Vascular endothelial growth factor up-regulates cyclooxygenase-2 expression in human endothelial cells. *J Clin Endocrinol Metab* **87:**3504–3507.
Teng J, Wang ZY, and Bjorling DE (2002) Estrogen-induced proliferation of urothelial cells is modulated by nerve growth factor. *Am J Physiol Renal Physiol* **282:** F1075–F1083.
Weiss RM (1998) Physiology and pharmacology of the renal pelvis and ureter, in *Campbell's Urology* (Walsh PC, Retik AB, Vaughan ED, Wein A eds) pp 839–869, WB Saunders, Philadelphia.
Yamamoto K. Arakawa T. Ueda N, and Yamamoto S (1995) Transcriptional roles of nuclear factor κB and nuclear factor-interleukin-6 in the tumor necrosis factor α-dependent induction of cyclooxygenase-2 in MC3T3–E1 cells. *J Biol Chem* **270:** 31315–31320.

**Address correspondence to:** Dr. Travis J. Jerde, University of Wisconsin Medical School, Department of Surgery, Division of Urology, K6-561 Clinical Science Center; 600 Highland Avenue, Madison, WI 53792. E-mail: jerde@surgery.wisc.edu